THE JOURNAL OF BIOLOGICAL CHEMISTRY VOL. 287, NO. 53, pp. 44221–44233, December 28, 2012

Involvement of *GDH3*-encoded NADP$^+$-dependent Glutamate Dehydrogenase in Yeast Cell Resistance to Stress-induced Apoptosis in Stationary Phase Cells*

Received for publication, April 24, 2012, and in revised form, October 12, 2012 Published, JBC Papers in Press, October 26, 2012, DOI 10.1074/jbc.M112.375360

Yong Joo Lee[1,2], **Kyung Jin Kim**[1], **Hong Yong Kang, Hye-Rim Kim, and Pil Jae Maeng**[3]

From the Department of Microbiology and Molecular Biology, Chungnam National University, Daejeon 305–764, Korea

Background: Gdh1 and Gdh3 are glutamate-synthesizing isofunctional NADP-GDH in *S. cerevisiae*.
Results: Stationary phase-specific *GDH3* expression and degradation of Gdh1 were responsible for the Gdh3-dependent glutamate supply and resistance to stress-induced apoptosis in stationary phase.
Conclusion: Gdh3 plays a role distinct from Gdh1 by rendering cells resistant to stress and aging.
Significance: This provides mechanistic insight into apoptosis and protein degradation in response to stress.

Glutamate metabolism is linked to a number of fundamental metabolic pathways such as amino acid metabolism, the TCA cycle, and glutathione (GSH) synthesis. In the yeast *Saccharomyces cerevisiae*, glutamate is synthesized from α-ketoglutarate by two NADP$^+$-dependent glutamate dehydrogenases (NADP-GDH) encoded by *GDH1* and *GDH3*. Here, we report the relationship between the function of the NADP-GDH and stress-induced apoptosis. Gdh3-null cells showed accelerated chronological aging and hypersusceptibility to thermal and oxidative stress during stationary phase. Upon exposure to oxidative stress, Gdh3-null strains displayed a rapid loss in viability associated with typical apoptotic hallmarks, *i.e.* reactive oxygen species accumulation, nuclear fragmentation, DNA breakage, and phosphatidylserine translocation. In addition, Gdh3-null cells, but not Gdh1-null cells, had a higher tendency toward GSH depletion and subsequent reactive oxygen species accumulation than did WT cells. GSH depletion was rescued by exogenous GSH or glutamate. The hypersusceptibility of stationary phase Gdh3-null cells to stress-induced apoptosis was suppressed by deletion of *GDH2*. Promoter swapping and site-directed mutagenesis of *GDH1* and *GDH3* indicated that the necessity of *GDH3* for the resistance to stress-induced apoptosis and chronological aging is due to the stationary phase-specific expression of *GDH3* and concurrent degradation of Gdh1 in which the Lys-426 residue plays an essential role.

Glutamate dehydrogenase (GDH)[4] (EC 1.4.1.3) catalyzes the reversible oxidative deamination of glutamate to α-ketoglutarate and ammonia using NAD(H) and NADP(H) as cofactors. The enzyme is present in almost all living organisms and plays a pivotal role in important cellular processes, such as the tricarboxylic acid (TCA), ammonia management, and energy metabolism (1). Although the equilibrium of mammalian GDH reaction favors the synthesis of glutamate, this reaction hardly occurs in mammalian cells because it requires high ammonia (K_m = 12–25 mM) and α-ketoglutarate (K_m = 1.0–2.0 mM) levels not likely to be seen under base-line conditions (1–3). When a high ammonia concentration prevails, however, glutamate synthesis via reductive amination of α-ketoglutarate by GDH may function as a detoxification process (4). The generation of α-ketoglutarate via oxidative deamination of glutamate leads to the production of NAD(P)H, GTP, and ATP through the TCA cycle in mitochondria. Therefore, GTP and ATP are allosteric inhibitors of GDH, whereas ADP is an activator (5).

In all mammals, except for humans and some closely related species, GDH is encoded by a single gene. However, humans and other primates have two distinct genes, *GLUD1* and *GLUD2*, that encode two isoforms of GDH, hGDH1 and hGDH2, respectively (6, 7). *GLUD1* is widely expressed in almost all human tissues including liver, brain, pancreas, and kidney, but not muscle. In pancreatic β-cells, immoderate generation of α-ketoglutarate due to an activating mutation of hGDH1 leads to increased insulin exocytosis through ATP overproduction (8–10). The activity of hGDH1 in β-cells is repressed by ADP-ribosylation catalyzed by SIRT4, one of seven homologs of yeast Sir2, which subsequently results in the down-regulation of insulin secretion (11). *GLUD2* is expressed predominantly in a limited range of tissues including retina, brain, and testis (7). Despite the high similarity between hGDH1 and hGDH2, as they share all but 16 of their 505 amino acid residues, they show definite differences in their basic catalytic activities and allosteric regulation (3, 5, 12, 13). Thus, the enzymes may contribute differentially to cellular processes. Deregulation of the activity of hGDH2 caused by an S445A substitution in the regulatory domain enhances glutamate oxidation, which results in enhanced nigral cell degeneration (14).

In contrast to mammals in which the reductive amination of α-ketoglutarate by GDH does not occur to an appreciable

* This work was supported by Grant 2009–0077095 from the National Research Foundation of Korea funded by the Ministry of Education, Science, and Technology (MEST).
[1] These authors contributed equally to this work.
[2] Present address: Dept. of Biochemistry and Molecular Biology Louisiana State University Health Science Ctr., 1501 Kings Hwy., Shreveport, LA 71130-3932.
[3] To whom correspondence should be addressed. Tel.: 82-42-821-6415; Fax: 82-42-822-7367; E-mail: pjmaeng@cnu.ac.kr.
[4] The abbreviations used are: GDH, glutamate dehydrogenase; NADP-GDH, NADP$^+$-dependent GDH; CFU, colony-forming unit; DCFH-DA, 2′,7′-dichlorodihydrofluorescein diacetate; GPx, glutathione peroxidase; PI, propidium iodide; ROS, reactive oxygen species; SCD, synthetic complete dextrose.

TABLE 1
***S. cerevisiae* strains and plasmids used in this study**

Strain and plasmid	Relevant genotype	Source
BY4741	*MATa his3Δ1 leu2Δ0 met15Δ0 ura3Δ0*	ATCC
BY4741-YOR375C	*Δgdh1::KanMX4 MATa his3Δ1 leu2Δ0 met15Δ0 ura3Δ0*	ATCC
BY4741-YDL215C	*Δgdh2::KanMX4 MATa his3Δ1 leu2Δ0 met15Δ0 ura3Δ0*	ATCC
BY4741-YAL062W	*Δgdh3::KanMX4 MATa his3Δ1 leu2Δ0 met15Δ0 ura3Δ0*	ATCC
MCBY004	*Δgdh3::URA3 Δgdh1::KanMX4 MATa his3Δ1 leu2Δ0 met15Δ0 ura3Δ0*	This study
MCBY005	*Δgdh3::URA3 Δgdh2::KanMX4 MATa his3Δ1 leu2Δ0 met15Δ0 ura3Δ0*	This study
MCBY006	*Δgdh1::URA3 Δgdh2::KanMX4 MATa his3Δ1 leu2Δ0 met15Δ0 ura3Δ0*	This study
YCpGdh1	*GDH1 LEU2*	This study
YCpGdh3	*GDH3 LEU2*	This study
$YCpP_{GDH1}$-Gdh3	$gdh1_P$::$gdh3_{ORF}$ *LEU2*	This study
$YCpP_{GDH3}$-Gdh1	$gdh3_P$::$gdh1_{ORF}$ *LEU2*	This study
YEpGdh2	*GDH2 URA3*	This study
$YEpP_{GDH1}$-LacZ	$gdh1_P$::*LACZ URA3*	This study
$YEpP_{GDH3}$-LacZ	$gdh3_P$::*LACZ URA3*	This study
YCpGdh1-FLAG	*GDH1::FLAG LEU2*	This study
YCpGdh3-FLAG	*GDH3::FLAG LEU2*	This study
$YCpP_{GDH1}$-Gdh3-FLAG	$gdh1_P$::$gdh3_{ORF}$::*FLAG LEU2*	This study
$YCpP_{GDH3}$-Gdh1-FLAG	$gdh3_P$::$gdh1_{ORF}$::*FLAG LEU2*	This study

extent, the yeast *Saccharomyces cerevisiae* cannot only biosynthesize glutamate but also utilize it via the reactions catalyzed by three distinct GDH isoenzymes. The NAD^+-dependent GDH (NAD-GDH; Gdh2) encoded by *GDH2* catalyzes reversible oxidative deamination of glutamate to α-ketoglutarate and ammonia (15). Glutamate anabolism via amination of α-ketoglutarate is catalyzed by two different $NADP^+$-dependent GDH (NADP-GDH), Gdh1 and Gdh3, encoded by *GDH1* and *GDH3*, respectively (16). Yeast cells lacking Gdh2 show impaired glutamate utilization and poor growth in minimal glucose media containing glutamate as a nitrogen source (15). Although Gdh2 is responsible for the reversible deamination of glutamate, it is not involved in glutamate biosynthesis during normal growth (15). On the contrary, Gdh1 and Gdh3 catalyze glutamate biosynthesis through the reductive amination of α-ketoglutarate (16). An alternative pathway for glutamate biosynthesis is accomplished by the combined activities of *GLN1*-encoded glutamine synthetase and the *GLT1*-encoded glutamate synthase (17, 18). However, both *GDH3* and *GLT1* are dispensable for yeast growth in minimal glucose medium containing ammonia as a sole nitrogen source, indicating that Gdh1 is the primary enzyme for glutamate biosynthesis (16). Gdh1 uses α-ketoglutarate at a higher rate than does Gdh3 and almost solely contributes to the NADP-GDH activity under fermentative growth conditions with glucose as the sole carbon source. However, during post-diauxic growth, the Gdh1/Gdh3 ratio decreases, and the majority of the total NADP-GDH activity is due to Gdh3, even though *GDH1* transcription proceeds during this growth phase (19). This phenomenon is in accordance with a previous observation in that NADP-GDH is degraded during glucose starvation (20).

In the present study, we examined the differential roles of two NADP-GDH, Gdh1 and Gdh3, in sustaining stress resistance. Our results indicate that Gdh3, but not Gdh1, is responsible for tolerance to stress-induced apoptosis in stationary phase cells, as there is stationary phase-specific expression of *GDH3* and degradation of Gdh1.

EXPERIMENTAL PROCEDURES

Yeast Strains, Media, and Transformation—S. cerevisiae strains used in this study are listed in Table 1. The YPD medium consisted of 1% yeast extract, 2% peptone, 75 μM adenine sulfate, and 2% glucose. The synthetic complete dextrose (SCD) medium consisted of 0.67% yeast nitrogen base without amino acids (Difco, Detroit, MI), 0.14% yeast synthetic drop-out medium supplement without leucine and uracil (Sigma-Aldrich), and 2% glucose. When necessary, SCD was supplemented with 2 mM uracil and 1 mM amino acids (glutamate and leucine). For solid media, 2% agar (Difco) was added. Transformation of yeast strains was performed using the lithium acetate method (21).

Plasmids—Plasmids used in this study are listed in Table 1. For construction of YCpGdh1, a 2.4-kb DNA fragment containing the promoter and coding sequence of *GDH1* was PCR-amplified from the genomic DNA of an *S. cerevisiae* WT strain (BY4741) with the primers P1-1 and P1-2 (Table 2). The resulting fragment was cloned into the low copy yeast/*Escherichia coli* shuttle vector YCp111. In parallel, to construct YCpGdh3, a 2.4-kb fragment containing the complete *GDH3* gene was PCR-amplified with the primers P3-1 and P3-2 (Table 2) and cloned into YCP111. To construct YEpGdh2, a 4.3-kb fragment containing the complete *GDH2* gene was amplified by PCR with the primers P2-1 and P2-2 (Table 2) and cloned into the high copy yeast/*E. coli* shuttle vector YEp352.

Two chimeric genes were constructed by a reciprocal exchange of the *GDH1* and *GDH3* promoter regions. For construction of $YCpP_{GDH1}$-Gdh3, a 1.0-kb fragment containing the promoter region of *GDH1* ($gdh1_P$) was PCR-amplified with the primers P1-1 and P1-3 (Table 2). A 1.4-kb fragment containing the complete coding sequence of Gdh3 ($gdh3_{ORF}$) was amplified with the primers P3-3 and P3-2 (Table 2). The two PCR products were fused by overlapping PCR, and the resulting 2.4-kb PCR product ($gdh1_P$::$gdh3_{ORF}$) was cloned into YCp111 to yield $YCpP_{GDH1}$-Gdh3. Similarly, for construction of $YCpP_{GDH3}$-Gdh1, a 1.0-kb fragment containing the promoter region of *GDH3* ($gdh3_P$) was amplified with the primers P3-1 and P3-4 (Table 2). A 1.4-kb fragment containing the complete coding sequence of Gdh1 ($gdh1_{ORF}$) was amplified with the primers P1-4 and P1-2 (Table 2). The two PCR products were combined by overlapping PCR, and the resulting 2.4-kb PCR

product (*gdh3*$_P$::*gdh1*$_{ORF}$) was cloned into YCp111 to yield YCpP$_{GDH3}$-Gdh1.

The genes coding for FLAG-tagged derivatives of Gdh1 and Gdh3 were constructed as follows. A 2.3-kb PCR fragment containing the promoter and coding region of *GDH1* followed by a FLAG-coding sequence was amplified with the primers P1-5 and P1-6 (Table 2) and cloned into YCp111 to yield YCpGdh1-FLAG. A 2.6-kb PCR fragment containing the promoter and coding region of *GDH3* followed by the FLAG-coding sequence was amplified with the primers P3-5 and P3-6 (Table 2) and cloned into YCp111 to yield YCpGdh3-FLAG.

The FLAG-tagged hybrid genes derived from *GDH1* and *GDH3* by promoter swapping were constructed as follows. A 2.4-kb DNA fragment containing the FLAG-tagged derivative of the *gdh1*$_P$::*gdh3*$_{ORF}$ hybrid (*gdh1*$_P$::*gdh3*$_{ORF}$::*FLAG*) was PCR-amplified from YCpP$_{GDH1}$-Gdh3 with the primers P1-1 and P3-7 (Table 2). The amplified fragment was cloned into YCp111 to yield YCpP$_{GDH1}$-Gdh3-FLAG. Similarly, the FLAG-tagged derivative of the *gdh3*$_P$::*gdh1*$_{ORF}$ hybrid gene (*gdh3*$_P$::*gdh1*$_{ORF}$::*FLAG*) was PCR-amplified from YCpP$_{GDH3}$-Gdh1 with the primers P3-8 and P1-6 (Table 2) and cloned into YCp111 to yield YCpP$_{GDH3}$-Gdh1-FLAG.

To construct the LacZ reporter plasmids for analysis of the expression of *GDH1* and *GDH3*, the promoter regions and short N-terminal coding sequences (6–8 amino acids) of *GDH1* (*gdh1*$_{P'}$) and *GDH3* (*gdh3*$_{P'}$) were fused in-frame to the *lacZ* gene. A 0.9-kb *gdh1*$_{P'}$ fragment was PCR-amplified with the primers P1-7 and P1-8 (Table 2). The resulting PCR product was fused in-frame to a promoter-less *lacZ* gene to construct the *gdh1*$_{P'}$::*lacZ* fusion in YEp353 (YEpP$_{GDH1}$-LacZ). In parallel, a 1.2-kb DNA fragment containing the *gdh3*$_{P'}$ fragment was PCR-amplified with the primers P3-5 and P3-9 (Table 2). The PCR fragment was then fused in-frame to a promoter-less *lacZ* gene to form a *gdh3*$_{P'}$::*lacZ* fusion in YEp353 (YEpP$_{GDH3}$-LacZ).

Site-directed Mutagenesis—Point mutations resulting in single amino acid substitutions in Gdh1 (K419A, K420A, K423A, and K426A) were introduced directly into the YCpGdh1-FLAG vector harboring the *GDH1* gene followed by the FLAG-coding sequence to yield YCpGdh1$_{K419A}$-FLAG, YCpGdh1$_{K420A}$-FLAG, YCpGdh1$_{K423A}$-FLAG, and YCpGdh1$_{K426A}$-FLAG. Site-directed mutagenesis was performed using a QuikChange II XL site-directed mutagenesis kit (Agilent, Santa Clara, CA) according to the manufacturer's instructions. The mutagenic oligonucleotide primers are as listed in Table 2: for K419A mutation, P1-419s and P1-419a; for K420A mutation, P1-420s and P1-420a; for K423A mutation, P1-423s and P1-423a; and for K426A mutation, P1-426s and P1-426s. All mutations were verified by sequencing to confirm that only the intended mutations had been introduced.

Gene Disruption—For construction of the Δ*gdh1*Δ*gdh3* and Δ*gdh2*Δ*gdh3* double mutants, a 1.8-kb DNA fragment containing Δ*gdh3*::*URA3* fusion construct was amplified by double-joint PCR with the following primers: for the 5′ flanking region of *GDH3*, P3-10 and P3-11; for the 3′ flanking region of *GDH3*, P3-12 and P3-13; for the *URA3* gene, P4-1 and P4-2; and for the final PCR round, P3-14 and P3-15 (Table 2). The Δ*gdh1* (BY4741-YOR375C) and Δ*gdh2* (BY4741-YDL215C) mutants were transformed with the Δ*gdh3*::*URA3* fusion construct to yield the Δ*gdh1*Δ*gdh3* (MCBY004) and Δ*gdh2*Δ*gdh3* (MCBY005) strains, respectively. Similarly, to construct the Δ*gdh1*Δ*gdh2* double mutant, a 1.8-kb PCR product containing the Δ*gdh1*::*URA3* fusion construct was amplified by double-joint PCR with the following primers: for the 5′ flanking region of *GDH1*, P1-9 and P1-10; for the 3′ flanking region of *GDH1*, P1-11 and P1-12; for the *URA3* gene, P4-1 and P4-2; and for the final PCR round, P1-13 and P1-14 (Table 2). The Δ*gdh2* mutant cells were then transformed with the Δ*gdh3*::*URA3* fusion construct to yield the Δ*gdh1*Δ*gdh2* (MCBY006) strain.

Survival Tests—For cell survival experiments, yeast cells were grown in SCD broth at 30 °C for 2 days (unless otherwise indicated) and suspended in PBS to a concentration of 1.0×10^8 cells ml^{-1}. Two-milliliter samples were taken and subjected to heat (50 °C, 30 min) or oxidative stress (1 mM H_2O_2, 1 h). One hundred-microliter aliquots of each sample were taken and serially diluted with 10-fold steps. For the colony-forming unit (CFU) assay, a 100-μl aliquot of each dilution was spread onto an SCD plate, and colonies were scored after incubation at 30 °C for 3 days.

Test for Apoptotic Markers—TUNEL assays were performed as described by Madeo *et al.* (22). In brief, cells were fixed with 3.7% formaldehyde, digested with lyticase (Sigma-Aldrich), applied to a polylysine-coated slide, treated with 0.3% H_2O_2 to block endogenous peroxidases, permeabilized with 0.1% Triton X-100, incubated with 10 μl of TUNEL reaction mixture (Roche Diagnostics) for 60 min at 37 °C, and incubated with 10 μl of Converter POD (Roche Diagnostics) for 10 min. A coverslip was mounted with a drop of Kaiser's glycerol gelatin (Merck, Darmstadt, Germany). Bright-field images of cells were acquired using a BX51 universal research microscope (Olympus Corp., Tokyo) equipped with a DP11 digital camera (Olympus).

To monitor the levels of intracellular reactive oxygen species (ROS), cells were stained with 10 μg ml^{-1} 2′,7′-dichlorodihydrofluorescein diacetate (DCFH-DA) for 2 h with shaking at 30 °C (23). For analysis of nuclear fragmentation, cells were fixed in 3.7% formaldehyde and stained with 0.5 μg ml^{-1} DAPI (Sigma-Aldrich) (22). Externalization of phosphatidylserine was assayed using FITC-coupled annexin V (BD Biosciences) as described by Madeo *et al.* (22). Cells were suspended in digestion buffer, and cell walls were digested as described above. The spheroplasts were stained with both FITC-annexin V and 500 μg ml^{-1} propidium iodide (PI; BD Biosciences).

Fluorescence microscopy was performed under a BX51 universal research microscope (Olympus) equipped with a DP11 digital camera (Olympus) using the appropriate filter sets (FITC filter for DCFH-DA and FITC-annexin V; DAPI filter for DAPI; and rhodamine filter for PI staining). To determine the frequencies of morphological phenotypes (TUNEL, DCFH-DA, DAPI, FITC-annexin V, and PI), at least 300 cells from three independent experiments were evaluated.

NADP-GDH and β-Gal Assay—To prepare whole cell extracts for NADP-GDH assays, yeast cells grown in liquid medium were harvested by centrifugation and washed twice with distilled water and once with extraction buffer (0.1 M potassium phosphate (pH 7.5), 1 mM EDTA, 1 mM DTT, 1 mM

TABLE 2
Oligonucleotide primers used in this study

Primer	Oligonucleotide sequence (5′-3′)
P1-1	GGATCCAAGAATGACAGCTTCCCAAG[a]
P1-2	GGATCCTTAAAATACATCACCTTG[a]
P1-3	aactatggttcgcttgtcatTTCTTTTTCTTTTTGGTCTC[b]
P1-4	gaaaaggtaaaaagtaaaaaATGTCAGAGCCAGAATTTCAA[c]
P1-5	GAGCTCCGAAAACTTCTCTTAATGATG[a]
P1-6	GAGCTCtcagatcttatcgtcgtcatccttgtaatcAAATACATCACCTTGGTCAAA[a,d]
P1-7	AAGCTTCGAAACTTCTCTTAATGATG
P1-8	AAGCTTGTTGAAATTCTGGCTCTGACAT[a]
P1-9	GGCATCGTTTACGATTGGCT
P1-10	ttatatgtagctttcgacatTTCTTTTT CTTTTTGGTCTC[e]
P1-11	gatgcggccagcaaaactaa ATAGTCTAAAAGAAAGAAAA[e]
P1-12	AGACATGAGAATTGTCAAAG
P1-13	GAATTCATACGGGTTGGCTGCTGGTA[a]
P1-14	GAATTCGGTTCCATGACTCCATGGAA[a]
P1-419s	CAATGAATGTATCGACTATGCC[underln]**GCG**AAGTACACTAAGGACGGTAAG[f]
P1-419a	CTTACCGTCCTTAGTGTACTT[underln]**CGC**GGCATAGTCGATACATTCATTG [f]
P1-420s	AATGTATCGACTATGCCAAG[underln]**GCG**TACACTAAGGACGGTAAGG [f]
P1-420a	CCTTACCGTCCTTAGTGTA[underln]**CGC**CTTGGCATAGTCGATACATT[f]
P1-423s	TATCGACTATGCCAAGAAGTACACT[underln]**GCG**GACGGTAAGGTC[f]
P1-423a	GACCTTACCGTC[underln]**CGC**AGTGTACTTCTTGGCATAGTCGATA[f]
P1-426a	AGAAGTACACTAAGGACGGT[underln]**GCG**GTCTTGCCATCTTTGGT[f]
P1-426s	ACCAAAGATGGCAAGAC[underln]**CGC**ACCGTCCTTAGTGTACTTCT[f]
P2-1	GAGCTCGAGCACTTGACGTTTGGTCC[a]
P2-2	GAGCTCTCAAGCACTTGCCTCCGCTT[a]
P3-1	GGATCCTAAAAACCGTCAAGGCAT[a]
P3-2	GGATCCCTAAAAAACGTCTCCCTGGT[a]
P3-3	gagaccaaaaagaaaaagaaATGACAAGCGAACCAGAGTT[g]
P3-4	tgaaattctggctctgacatTTTTTACTTTTTACCTTTTC[h]
P3-5	AAGCTTGCGGTTATATGATCTTC[a]
P3-6	AAGCTTtcagatcttatcgtcgtcatccttgtaatcAAAAACGTCTCCCTGGTCAAG[a,d]
P3-7	GGATCCtcagatcttatcgtcgtcatccttgtaatcAAAAACGTCTCCCTGGTCAAG[a,d]
P3-8	GAGCTCTAAAAACCGTCAAGGCAT[a]
P3-9	AAGCTTCTGGTTCGCTTGTCAT[a]
P3-10	TAAACATACTTGTGGCAGCT
P3-11	ttatatgtagctttcgacatTTTTTACTTTTTACCTTTTC[e]
P3-12	gatgcggccagcaaaactaaCCGTAAGCGCTATTTTCTTT[e]
P3-13	AATCACAAGCTCATCGGGCG
P3-14	GAATTCGAGCACTTGCCAAAGTAATT[a]
P3-15	GAATTCTATGTTCAATGAATTTATTG[a]
P4-1	ATGTCGAAAGCTACATATAA
P4-2	TTAGTTTTGCTGGCCGCATC

[a] Underlined small capitals indicate additional restriction sites.
[b] Lowercase letters indicate additional Gdh3 N-terminal coding sequence.
[c] Lowercase letters indicate additional *GDH3* promoter region.
[d] Lowercase letters indicate additional FLAG-coding sequence.
[e] Lowercase letters indicate additional *URA3* sequence.
[f] Underlined bold capitals indicate mutations (Lys → Ala) incorporated into the primers.
[g] Lowercase letters indicate additional *GDH1* promoter region.
[h] Lowercase letters indicate additional N-terminal coding sequence for Gdh1.

PMSF, and 50 μl ml^{-1} *N*-α-*p*-tosyl-L-lysine chloromethyl ketone) (24). Cell pellets were stored at −20 °C. Soluble extracts were prepared by mechanical disruption of cells suspended in extraction buffer by agitation with glass beads in a vortex mixer (five cycles of 1 min of agitation and 1 min of incubation on ice) followed by brief centrifugation to clarify the lysate. NADP-GDH activity was assayed by measuring the oxidation of NADPH according to the method of Doherty (25). One unit of NADP-GDH activity corresponds to 1 μmol of $NADP^+$ produced/min. Protein was measured by the method of Lowry *et al.* (26) using BSA as a standard.

β-Gal assays were performed using a yeast β-gal assay kit (Thermo Scientific) according to the manufacturer's instructions. β-Gal activity was calculated using the following equation: β-gal activity = $(1000 \times A_{420})/(t \times V \times OD_{660})$ in which t = time (in minutes) of incubation and V = volume of cells (ml) used in the assay.

Glutathione and Glutamate Assays—Intracellular levels of the total glutathione pool, glutathione (GSH) and glutathione disulfide (GSSG), were determined by measuring the rate of 2-nitro-5-thiobenzoic acid formation from 5,5′-dithiobis-(2-nitrobenzoic acid) (Sigma-Aldrich) in the glutathione recycling system (27). Five microliters of cell lysate was added to 1 ml of 100 mM phosphate buffer (pH 7.5) containing 0.6 mM 5,5′-dithiobis-(2-nitrobenzoic acid), 5 mM EDTA, 0.2 mM NADPH, and 1 unit ml^{-1} glutathione reductase (Sigma-Aldrich). The rate of increase in A_{412} was monitored. To determine the levels of GSSG, NADPH consumption was monitored by measuring the rate of decrease in A_{340}. Intracellular levels of glutamate were determined using a colorimetric glutamate analysis kit (R-Biopharm, Darmstadt, Germany) according to manufacturer's instructions.

Immunoblotting—To prepare cell extracts for immunoblotting, 1×10^9 cells suspended in 50 μl of lysis buffer (0.5% Nonidet P-40, 20 mM HEPES (pH 7.4), 84 mM KCl, 10 mM $MgCl_2$, 0.2 mM EDTA, 0.2 mM EGTA, 1 mM DTT, 5 μg ml^{-1} aprotinin, 1 μg ml^{-1} leupeptin, 1 μg ml^{-1} pepstatin, and 1 mM phenylmethylsulfonyl fluoride) were mechanically disrupted by agitation with glass beads in a vortex mixer. Proteins were separated by gradient SDS-PAGE and electroblotted onto a PVDF mem-

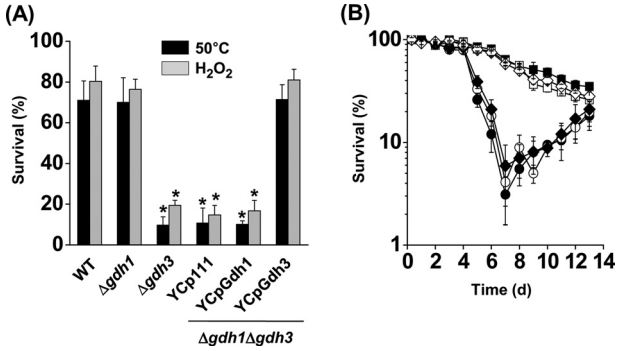

FIGURE 1. **Deletion of *GDH3* results in increased sensitivity of yeast cells to thermal, oxidative, and aging stress.** *A*, survival rates of yeast strains exposed to thermal or oxidative stress. Yeast cells (WT, Δ*gdh1*, Δ*gdh3*, Δ*gdh1*Δ*gdh3*/YCp111, Δ*gdh1*Δ*gdh3*/YCpGdh1, and Δ*gdh1*Δ*gdh3*/YCpGdh3) grown in SCD for 2 days were exposed to thermal (50 °C, 30 min) or oxidative (10 mM H_2O_2, 1 h) stress. Surviving cells were evaluated by CFU assays. Values are the means ± S.E. of three independent experiments. *, $p <$ 0.001 (two-tailed Student's *t* test *versus* WT). *B*, survival rates of yeast strains during chronological aging. The yeast strains listed in *A* were grown in SCD for 13 days. Surviving cells were evaluated as described in *A*. ■, WT; □, Δ*gdh1*; ●, Δ*gdh3*; ○, Δ*gdh1*Δ*gdh3*/YCp111; ◆, Δ*gdh1*Δ*gdh3*/YCpGdh1; ◇, Δ*gdh1*Δ*gdh3*/YCpGdh3.

brane (R-Biopharm). Blots were processed as described by Lauber *et al.* (28).

Gdh1 and Gdh3 proteins were probed with polyclonal anti-Gdh1 and anti-Gdh3 antibodies (Young In Frontier Co., Seoul, Korea) derived from rabbits immunized with the synthetic peptides CIDYAKKYTKDGKV and CIQAAQEYSTEKNTNT, respectively. FLAG-tagged proteins were probed with a rabbit polyclonal anti-FLAG antibody (Sigma-Aldrich). Tubulin, a loading control, was probed with a rabbit anti-tubulin antibody (Sigma-Aldrich). Membranes were then incubated with HRP-conjugated affinity-purified goat anti-rabbit secondary antibody (Sigma-Aldrich) followed by enhanced chemiluminescent staining using ECL reagents (R-Biopharm).

RESULTS

Deletion of GDH3 Causes Increased Sensitivity to Thermal and Oxidative Stress in Stationary Phase Cells and Accelerates Chronological Aging—To address the differential roles of the two NADP-GDH, Gdh1 and Gdh3, we examined the resistance against heat and oxidative stress of NADP-GDH yeast mutants and their derivatives that harbor either ectopically expressed *GDH1* or *GDH3* genes. Although the survival rates of the WT, Δ*gdh1*, and Δ*gdh1*Δ*gdh3*/YCpGdh3 yeast strains grown in SCD for 2 days were ~70% after 30 min of exposure to heat stress at 50 °C, less than 10% of the initial population of the Δ*gdh3* (BY4741-YAL062W), Δ*gdh1*Δ*gdh3*/YCp111, and Δ*gdh1*Δ*gdh3*/YCpGdh1 strains survived following the same treatment (Fig. 1*A*). In addition, only 10–15% of the initial population of Δ*gdh3*, Δ*gdh1*Δ*gdh3*/YCp111, and Δ*gdh1*Δ*gdh3*/YCpGdh1 cells cultured for 2 days survived after a 1-h exposure to 1 mM H_2O_2, whereas more than 75% of the WT, Δ*gdh1*, and Δ*gdh1*Δ*gdh3*/YCpGdh3 cells subjected to the same treatment remained alive. These results indicate that deletion of *GDH3* causes increased sensitivity to both heat and oxidative stress in stationary phase cells, whereas impairment of *GDH1* leads to no significant stress-sensitive phenotype. Additionally, the stress sensitivity of the Gdh3-null mutants was not suppressed by ectopic expression of *GDH1*.

Intracellular ROS is a mediator of chronological aging in yeast (29, 30). Accordingly, we have shown previously that ROS accumulation caused by depletion of intracellular glutamate in the yeast cells lacking Cit1, which catalyzes the first step of the TCA cycle, leads to accelerated chronological aging (31). To determine whether the deletion of *GDH1* or *GDH3* affects the survival of cells in chronologically aged yeast cultures, WT and mutant cells were cultured in SCD for 13 days, and the surviving cells were quantified by CFU assay. Although ~50% of the initial populations of the WT, Δ*gdh1*, and Δ*gdh1*Δ*gdh3*/YCpGdh3 strains remained viable after a 7-day culture, only 2–5% of the Δ*gdh3*, Δ*gdh1*Δ*gdh3*/YCp111, and Δ*gdh1*Δ*gdh3*/YCpGdh1 cells survived after the same culture period (Fig. 1*B*). In addition, the survival rates of Δ*gdh3*, Δ*gdh1*Δ*gdh3*/YCp111, and Δ*gdh1*Δ*gdh3*/YCpGdh1 cultures reached their minimum levels after 7 days and then increased continuously up to 20–30% of the initial population during a subsequent 6-day cultivation. This result indicates that the Gdh3-null strains experienced a much faster and more severe aging process than did their isogenic WT population. Furthermore, Gdh3-null cells were subjected to accelerated aging-dependent cell death followed by adaptive regrowth upon long-term cultivation. Our data support a previous study that reported that during the chronological aging process of yeast, premature apoptotic death promotes the regrowth of a subpopulation of better adapted mutants (29).

Oxidative Stress-induced Death of Stationary Phase Gdh3-null Cells Is Caused by ROS-mediated Apoptosis—To clarify whether the increased sensitivity of the Gdh3-null cells to heat and oxidative stress is caused by a higher tendency of the mutant populations toward stress-induced apoptosis, we looked for cytological and biochemical features of apoptosis in the mutant cells. We analyzed the cells for the presence of intracellular ROS, which are both necessary and sufficient for inducing apoptosis in yeast (32). As a probe for ROS production, we used DCFH-DA, which can be oxidized to the fluorescent chromophore 2′,7′-dichlorofluorescein primarily by the action of peroxide (H_2O_2). As seen in the fluorescence micrographs (Fig. 2, *A* and *D*), a vast majority of the Δ*gdh3* (72%) and Δ*gdh1*Δ*gdh3* cells (88%) grown for 2 days in SCD broth at 30 °C were fluorescent after a 1-h exposure to 10 mM H_2O_2. On the other hand, the WT and Δ*gdh1* cells did not show any detectable levels of 2′,7′-dichlorofluorescein fluorescence under these conditions. Therefore, these results indicate that deletion of *GDH3* causes oxidative stress-dependent accumulation of ROS in stationary phase cells.

Because Δ*gdh1* and Δ*gdh1*Δ*gdh3* cells exposed to oxidative stress have elevated ROS levels, we assayed for nuclear fragmentation, a well established cytological hallmark of apoptosis. A normal, single-round nucleus was detected by DAPI staining in WT and mutant cells under normal conditions (untreated) (Fig. 2, *B* and *D*). On the other hand, ~66 and 72% of the Δ*gdh3* and Δ*gdh1*Δ*gdh3* cells, respectively, displayed irregularly shaped and fragmented nuclei at 1 h after exposure to H_2O_2. In contrast, only ~20% of the similarly treated WT and Δ*gdh1* strains had abnormal nuclei.

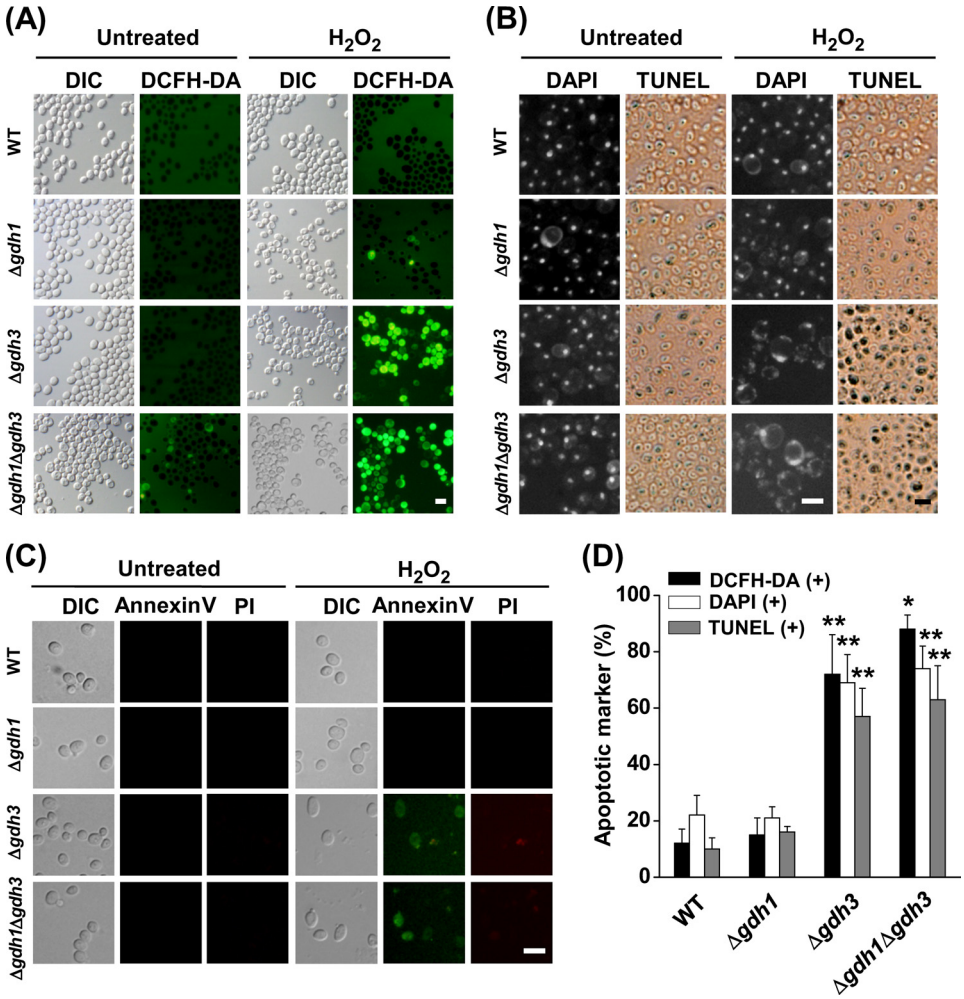

FIGURE 2. **Yeast Gdh3-null cells display apoptotic markers under stress conditions.** *A*, ROS accumulation in yeast cells exposed to oxidative stress. Yeast cells (WT, Δ*gdh1*, Δ*gdh3*, and Δ*gdh1*Δ*gdh3*) grown in SCD for 2 days were exposed to 10 mM H_2O_2 for 1 h. Cells were stained with DCFH-DA and examined by fluorescence microscopy. *Bar*, 10 μm. *DIC*, differential interference contrast. *B*, nuclear or DNA fragmentation in yeast cells exposed to oxidative stress. Yeast cells prepared and treated as described in *A* were stained with DAPI or TUNEL reagent and examined by fluorescence microscopy. *Bar*, 10 μm. *C*, phosphatidylserine externalization in yeast cells exposed to oxidative stress. Yeast strains prepared and treated as described in *A* were stained with FITC-annexin V and PI and examined by fluorescence microscopy. *Bar*, 10 μm. *D*, percentage of yeast cells exhibiting the typical hallmarks of apoptosis after exposure to oxidative stress (10 mM H_2O_2, 1 h). The number of cells with accumulated ROS (*DCFH-DA*(+)), fragmented nuclei (*DAPI*(+)), and fragmented DNA (*TUNEL*(+)) were determined from ~500–700 cells in three independent experiments. Values are the mean ± S.E. *, $p < 0.001$; **, $p < 0.005$ (two-tailed Student's *t* test *versus* WT).

We also examined nuclear DNA fragmentation, another feature of apoptosis, using TUNEL analysis in which fluorescent nucleotides were added to the 3′-OH ends of the DNA fragments making the phenomenon visible by fluorescence microscopy. None of the WT or mutant cells had TUNEL-positive nuclei under normal conditions (untreated) (Fig. 2, *B* and *D*). However, after 1 h of exposure to H_2O_2, ~58 and 62% of Δ*gdh3* and Δ*gdh1*Δ*gdh3* cells, respectively, showed intensely stained nuclei indicating DNA strand breakage. On the other hand, the nuclei of both the WT and Δ*gdh1* cells remained unstained or only slightly stained after the same treatment.

In yeast cells as well as mammalian cells, translocation of phosphatidylserine, which is predominantly located on the inner leaflet of the plasma membrane under normal conditions, to the outer leaflet serves as a sensitive marker for the early stages of apoptosis (33). For detection of phosphatidylserine in the outer layer of the cytoplasmic membrane, spheroplasts formed from the cells subjected to oxidative stress were stained with both FITC-annexin V and PI. The stained cells were then observed by fluorescence microscopy. When exposed to H_2O_2 for 1 h, a portion of the stationary phase cells from the Δ*gdh3* and Δ*gdh1*Δ*gdh3* strains were stained exclusively with FITC-annexin V, indicating that they were undergoing an early stage of apoptosis (Fig. 2*C*). In addition, some of the oxidatively stressed cells were dually stained with both FITC-annexin V and PI, suggesting the late apoptotic phases or necrosis. On the contrary, only a negligible portion of the similarly treated WT and Δ*gdh1* cells were stained solely with FITC-annexin V and thus were considered to be apoptotic. These results suggest that stationary phase Gdh3-null cells are much more susceptible to oxidative and thermal stress-induced cell death (bearing the structural attributes of apoptosis) than are the isogenic WT strains.

Stationary Phase Gdh3-null Cells Exhibit GSH and Glutamate Depletion, Which Leads to Increased Susceptibility to Oxidative Stress-induced Apoptosis—GSH synthesized from glutamate, glycine, and cysteine by the action of γ-glutamylcysteine

TABLE 3
Intracellular levels of GSH and glutamate in *S. cerevisiae* strains grown in different media

Strain	GSH[a] + additions to SCD			Glutamate[b] + additions to SCD		
	1 mM Glutamate	10 mM Glutamate	10 mM GSH	1 mM Glutamate	10 mM Glutamate	10 mM GSH
	nmol/mg protein			*nmol/mg protein*		
WT	121.4 ± 8.6	131.5 ± 10.6	137.3 ± 15.1	11.1 ± 3.3	19.6 ± 3.8	13.2 ± 4.6
Δ*gdh1*	118.7 ± 10.5	123.7 ± 5.8	139.4 ± 7.9	9.9 ± 2.2	18.9 ± 6.7	14.4 ± 3.3
Δ*gdh2*	125.9 ± 3.4	133.7 ± 11.5	134.5 ± 19.3	13.4 ± 4.4	22.6 ± 5.5	15.7 ± 2.1
Δ*gdh3*	31.7 ± 10.6	120.5 ± 18.3	105.1 ± 32.1	2.1 ± 0.7	17.4 ± 4.2	10.1 ± 4.2
Δ*gdh1*Δ*gdh2*	120.4 ± 5.8	125.7 ± 10.4	136.7 ± 4.7	11.5 ± 1.9	20.5 ± 0.8	16.2 ± 2.0
Δ*gdh1*Δ*gdh3*	35.1 ± 6.0	115.6 ± 10.1	110.6 ± 10.6	1.9 ± 0.7	16.8 ± 5.2	10.8 ± 1.1
Δ*gdh2*Δ*gdh3*	81.7 ± 19.1	124.6 ± 4.1	99.8 ± 4.6	6.1 ± 2.5	18.1 ± 3.8	12.5 ± 2.6

[a] Values were obtained from [(GSH + GSSG) − GSSG] and are presented as mean ± S.E. from three independent experiments. The percentage of GSSG to total cellular glutathione pool (GSH + GSSG) was <10% in all strains.
[b] Values are presented as mean ± S.E. from three independent experiments.

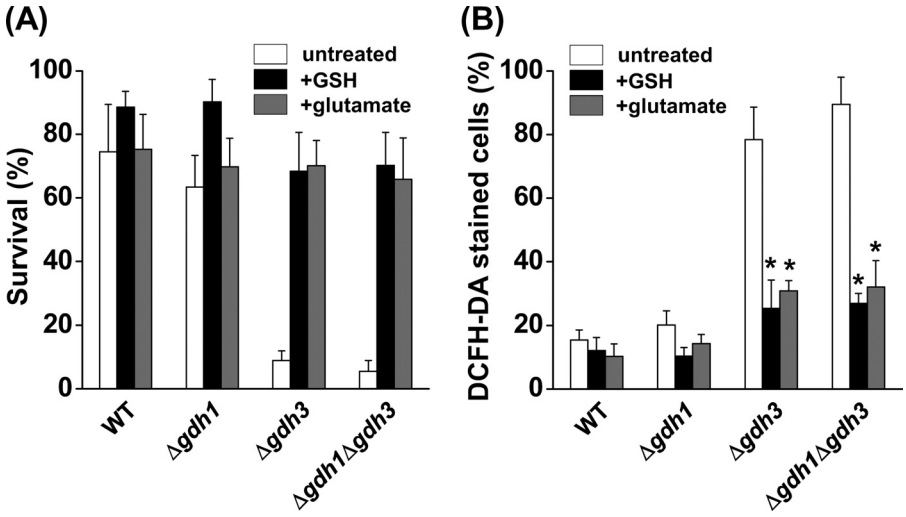

FIGURE 3. **Exogenous supply of GSH or glutamate suppresses the hypersusceptibility of yeast Gdh3-null cells to stress-induced apoptosis mediated by ROS accumulation.** *A*, effect of exogenous GSH and glutamate on survival of yeast cells exposed to oxidative stress. Yeast strains (WT, Δ*gdh1*, Δ*gdh3*, and Δ*gdh1*Δ*gdh3*) grown in SCD with or without 10 mM GSH or glutamate for 2 days were exposed to 10 mM H_2O_2 for 1 h. Surviving cells were evaluated by CFU assays. Values are the mean ± S.E. of three independent experiments. *B*, effect of exogenous GSH and glutamate on ROS accumulation in yeast cells exposed to oxidative stress. Yeast cells prepared and treated as described in *A* were stained with DCFH-DA and examined by fluorescence microscopy. The number of DCFH-DA-positive cells was estimated in fluorescence images and total cells in the corresponding differential interference contrast images. Approximately 500–700 cells were observed in three independent experiments. Values are the mean ± S.E. *, $p < 0.005$ (two-tailed Student's *t* test *versus* untreated).

synthase (Gsh1) and GSH synthase (Gsh2) is one of the most prevalent reducing thiol compounds functioning as an antioxidant in nearly every aerobic organism (34). Accordingly, depletion of GSH or its precursor, glutamate, causes oxidative or thermal stress-induced apoptosis in yeast cells (31).

To determine whether the ROS accumulation in stressed Gdh3-null cells is facilitated by depletion of GSH, which is used by many peroxidases to scavenge H_2O_2 and a multitude of organic hydroperoxides (35), we evaluated the levels of GSH in the mutant cells (Table 3). When Δ*gdh3* and Δ*gdh1*Δ*gdh3* cells were grown for 2 days in SCD containing 1 mM glutamate, the levels of GSH were ~26 and 29% of that in WT cells, respectively. In contrast, Δ*gdh3* and Δ*gdh1*Δ*gdh3* mutants exhibited GSH levels similar to those of WT cells when grown in SCD supplemented with a higher concentration of either glutamate or GSH (88 and 92% in the presence of 10 mM glutamate and 76 and 80% in the presence of 10 mM GSH, respectively). Accordingly, the intracellular levels of glutamate were similar to those of GSH. Glutamate concentrations in the cells of Δ*gdh3* and Δ*gdh1*Δ*gdh3* mutants were 20% less than that of WT cells when cultured in SCD containing 1 mM glutamate. The depletion of glutamate in Δ*gdh3* and Δ*gdh1*Δ*gdh3* mutant cells recovered to at least 75% of the normal level when the medium was supplemented with either 10 mM GSH or 10 mM glutamate.

We examined the effect of exogenous GSH and glutamate on stress-induced apoptosis of the yeast strains. In accordance with the restoration of the intracellular GSH and glutamate levels, Δ*gdh3* and Δ*gdh1*Δ*gdh3* cells grown in SCD medium supplemented with 10 mM GSH or glutamate showed almost the same level of survival after a 1-h exposure to 10 mM H_2O_2 as did WT and Δ*gdh1* cells (Fig. 3*A*). In addition, when stained with DCFH-DA, Δ*gdh3* and Δ*gdh1*Δ*gdh3* cells showed only slightly higher levels of DCF fluorescence compared with WT and Δ*gdh1* cells under oxidative stress conditions. This indicates significant attenuation of stress-induced ROS accumulation in the presence of 10 mM GSH or glutamate (Fig. 3*B*). Together, these data suggest that the deletion of *GDH3* results in the depletion of intracellular GSH, which, in turn, induces the accumulation of ROS and accompanying apoptotic cell death during stress conditions.

The Increased Susceptibility of Stationary Phase Gdh3-null Cells to Thermal and Oxidative Stress-induced Apoptosis Is Suppressed by GDH2 Deletion—The NAD-GDH (Gdh2) encoded by *GDH2* catalyzes oxidative deamination of gluta-

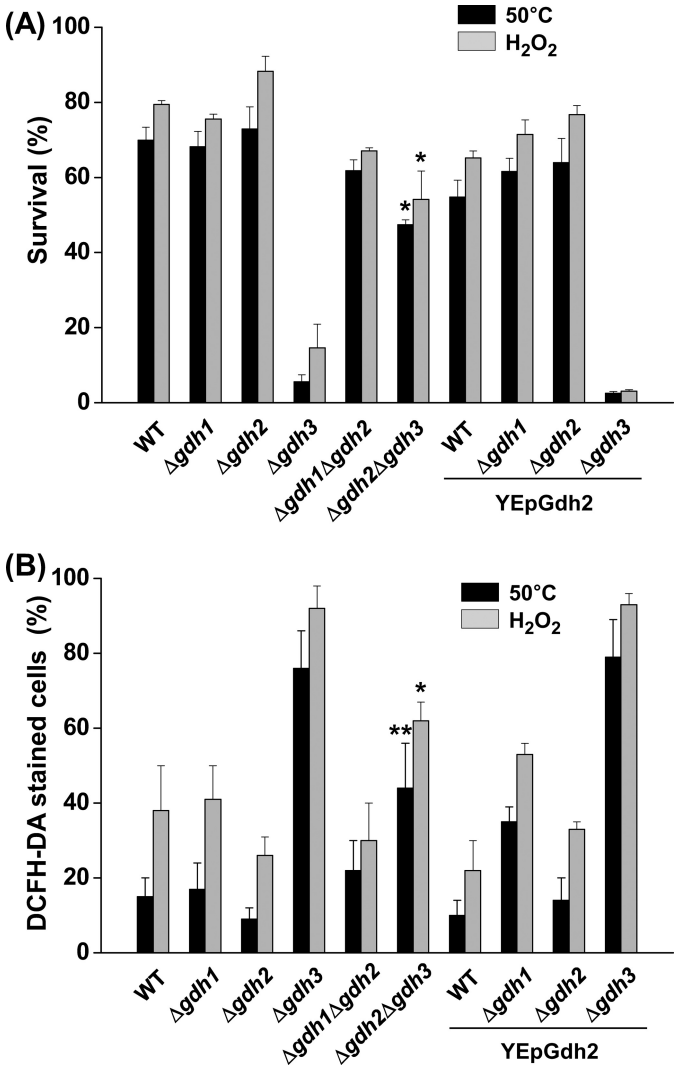

FIGURE 4. **Deletion of *GDH2* suppresses the hypersusceptibility of yeast Gdh3-null cells to stress-induced apoptosis mediated by ROS accumulation.** *A*, effect of Δ*gdh2* mutation on survival of yeast cells exposed to thermal or oxidative stress. Yeast strains (WT, Δ*gdh1*, Δ*gdh2*, Δ*gdh3*, Δ*gdh2*Δ*gdh3*, WT/YEpGDH2, Δ*gdh1*/YEpGDH2, Δ*gdh2*/YEpGDH2, and Δ*gdh3*/YEpGDH2) grown in SCD for 2 days were exposed to either thermal (50 °C, 30 min) or oxidative stress (10 mM H_2O_2, 1 h). Surviving cells were evaluated by CFU assays. Values are the means ± S.E. of three independent experiments. *, $p < 0.001$ (two-tailed Student's *t* test *versus* Δ*gdh3*). *B*, effect of the Δ*gdh2* mutation on ROS accumulation in yeast cells exposed to thermal or oxidative stress. Yeast cells prepared and treated as described in *A* were stained with DCFH-DA and examined by fluorescence microscopy. The number of DCFH-DA-positive cells was estimated in fluorescence images and total cells in corresponding differential interference contrast images. Approximately 500–700 cells were observed in three independent experiments. Values are the mean ± S.E. *, $p < 0.001$; **, $p < 0.05$ (two-tailed Student's *t* test *versus* Δ*gdh3*).

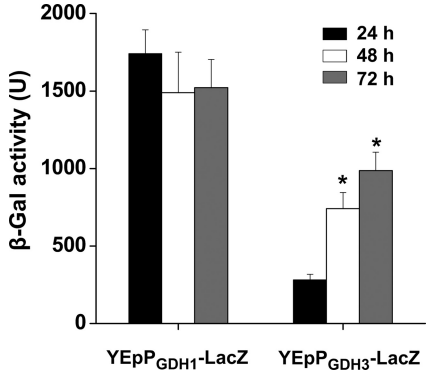

FIGURE 5. **GDH3 transcription occurs exclusively during stationary phase, whereas *GDH1* transcription is consistent throughout all growth periods.** Yeast strains (WT/$YEpP_{GDH1}$-LacZ and WT/$YEpP_{GDH3}$-LacZ) were grown in SCD, and samples were taken after 24, 48, and 72 h of culture. *GDH1* and *GDH3* transcription levels were estimated by measuring β-gal activity. β-Gal activity was calculated using the following equation: β-gal activity = $(1000 \times A_{420})/(t \times V \times OD_{660})$, where t = time (in minutes) of incubation and V = volume of cells (ml) used in the assay. Three independent experiments were performed in triplicate. Values are the mean ± S.E. *, $p < 0.001$ (two-tailed Student's *t* test *versus* $YEpP_{GDH3}$-LacZ at 24 h).

mate to α-ketoglutarate and ammonia (15), hence the reverse reaction of glutamate synthesis from α-ketoglutarate catalyzed by either Gdh1 or Gdh3. To investigate how Gdh2 function is related to stress-induced apoptosis, we analyzed the effect of *GDH2* deletion and the presence of ectopic *GDH2* on the hypersusceptibility of Gdh3-null mutants.

The introduction of the Δ*gdh2* mutation caused increased resistance to both thermal and oxidative stress in Gdh3-null strain (Fig. 4*A*). The survival rates of Δ*gdh2*Δ*gdh3* cells grown for 2 days in SCD were ~55% after a 1-h exposure to oxidative stress (10 mM H_2O_2) and 47% after a 30-min exposure to thermal stress (50 °C), whereas the survival rates of Δ*gdh3* cells were ~15 and 5%, respectively. Correspondingly, Δ*gdh2*Δ*gdh3* cells exposed to oxidative and thermal stress exhibited significantly lower levels of ROS accumulation (~44 and 62%, respectively) compared with Δ*gdh3* cells (~76 and 92%, respectively) when monitored by fluorescence microscopy using DCFH-DA (Fig. 4*B*). In addition, the levels of GSH and glutamate in Δ*gdh2*Δ*gdh3* cells were ~2.6- and 2.9-fold higher than that of Δ*gdh3* cells, respectively, when the cells were grown for 2 days in SCD containing a basal level of glutamate (1 mM) (Table 3). On the contrary, all of the yeast strains containing ectopic *GDH2* in high copy vectors (WT/YEpGdh2, Δ*gdh1*/YEpGdh2, Δ*gdh2*/YEpGdh2, and Δ*gdh3*/YEpGdh2) showed reduced resistance against both thermal and oxidative stress-induced apoptosis, although to a limited extent, compared with their corresponding host strains (Fig. 4*A*). Thus, it appears that deletion of *GDH2* compensates for the depletion of intracellular glutamate and GSH followed by stress-induced ROS accumulation and apoptotic cell death in stationary phase Gdh3-null cells, whereas ectopic expression of *GDH2* enhances the depletion of intracellular glutamate and GSH. These results are in agreement with the fact that Gdh2 catalyzes the oxidative deamination of glutamate to α-ketoglutarate resulting in decreased intracellular glutamate and GSH levels.

GDH1, but Not GDH3, Is Responsible for the Resistance against Stress-induced Apoptosis in Logarithmic Phase Cells—To determine the differential roles of *GDH1* and *GDH3* in sustaining resistance to stress-induced apoptosis, we monitored the ectopic expression of $gdh1_{P'}$::*lacZ* and $gdh3_{P'}$::*lacZ* hybrid genes in WT/$YEpP_{GDH1}$-LacZ and WT/$YEpP_{GDH3}$-LacZ strains, respectively. Considerably higher levels of β-gal activity (≥1500 units) were detected in the WT/$YEpP_{GDH1}$-LacZ cell extracts, regardless of the growth stage, than in the WT/$YEpP_{GDH3}$-LacZ cell extracts (Fig. 5). The level of β-gal activity in WT/$YEpP_{GDH3}$-LacZ cells was low (~250 units) after a 24-h culture into late logarithmic phase but gradually increased dur-

TABLE 4
Intracellular levels of NADP-GDH and NAD-GDH activities in *S. cerevisiae* strains

Strain	NADP-GDH-specific activity[a]		NAD-GDH-specific activity[a]	
	24 h[b]	48 h[b]	24 h[b]	48 h[b]
WT	1.224 ± 0.102	1.451 ± 0.126	0.042 ± 0.002	0.051 ± 0.003
Δ*gdh1*	0.121 ± 0.006	1.316 ± 0.092	0.039 ± 0.001	0.057 ± 0.003
Δ*gdh2*	1.213 ± 0.083	1.413 ± 0.117	<0.002	<0.002
Δ*gdh3*	1.144 ± 0.088	0.159 ± 0.054	0.048 ± 0.002	0.049 ± 0.004
Δ*gdh1*Δ*gdh2*	0.120 ± 0.090	1.307 ± 0.125	<0.002	<0.002
Δ*gdh1*Δ*gdh3*	<0.005	<0.005	0.045 ± 0.003	0.055 ± 0.005
Δ*gdh2*Δ*gdh3*	1.219 ± 0.099	0.234 ± 0.016	<0.002	<0.002
Δ*gdh1*Δ*gdh3*/YCpGdh1	1.145 ± 0.108	0.187 ± 0.013	0.044 ± 0.001	0.054 ± 0.002
Δ*gdh1*Δ*gdh3*/YCpGdh3	0.122 ± 0.009	1.345 ± 0.117	0.041 ± 0.003	0.052 ± 0.003
Δ*gdh1*Δ*gdh3*/YCpP_{GDH1}-Gdh3	1.253 ± 0.081	1.559 ± 0.089	0.047 ± 0.003	0.058 ± 0.004
Δ*gdh1*Δ*gdh3*/YCpP_{GDH3}-Gdh1	0.007 ± 0.001	0.222 ± 0.014	0.046 ± 0.004	0.053 ± 0.005

[a] Values given in μmol/min/mg protein and presented as mean ± S.E. from three independent experiments.
[b] Length of time cells were cultured in SCD.

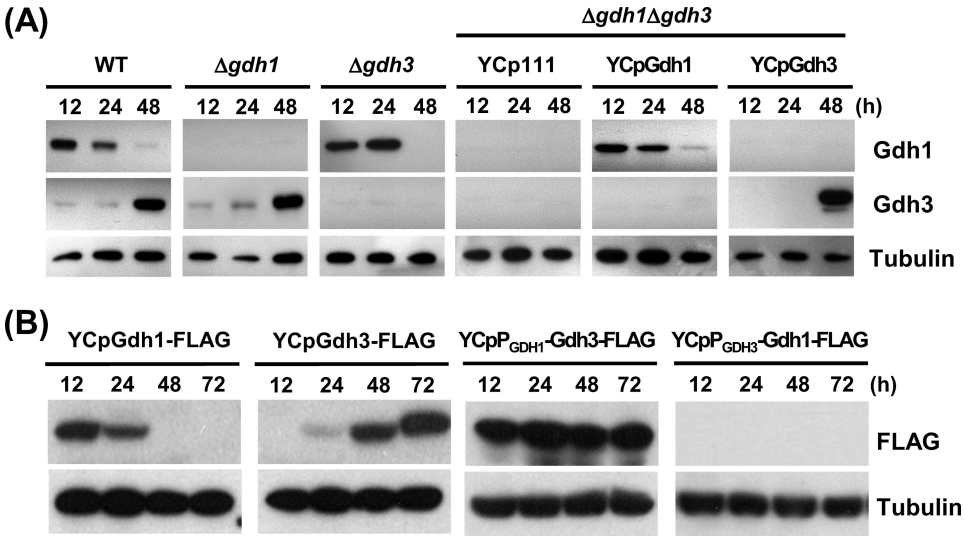

FIGURE 6. **Gdh3 protein is stable throughout all growth stages, whereas Gdh1 is subjected to stationary phase-specific degradation.** *A*, immunoblot analysis of the Gdh1 and Gdh3 proteins in yeast cells at different growth stages. Yeast strains (WT, Δ*gdh1*, Δ*gdh3*, Δ*gdh1*Δ*gdh3*/YCp111, Δ*gdh1*Δ*gdh3*/Gdh1, Δ*gdh1*Δ*gdh3*/YCpGdh3) were grown in SCD, and samples were taken after 24 and 48 h of culture. Cell extracts were immunoblotted and probed with anti-Gdh1, anti-Gdh3 and anti-tubulin antibodies. *B*, immunoblot analysis of the FLAG-tagged Gdh1 and Gdh3 proteins in yeast cells carrying the promoter-swapped derivatives of *GDH1* and *GDH3* at different growth stages. Yeast strains (Δ*gdh1*Δ*gdh3*/YCpGdh1-FLAG, Δ*gdh1*Δ*gdh3*/YCpGdh3-FLAG, Δ*gdh1*Δ*gdh3*/YCpP_{GDH1}-Gdh3-FLAG, and Δ*gdh1*Δ*gdh3*/YCpP_{GDH3}-Gdh1-FLAG) were grown in SCD and samples were taken after 12, 24, 48, and 72 h of culture. Cell extracts were immunoblotted and probed with anti-FLAG and anti-tubulin antibodies.

ing the following 48-h period up to levels 4-fold higher than during the logarithmic phase (~1,000 units). Therefore, *GDH1* was expressed consistently throughout all of the growth periods at a relatively high level, whereas *GDH3* was expressed at negligible levels during the logarithmic phase but increased gradually to a higher level during stationary phase. These results are in agreement with a previous report indicating that *GDH3* transcription is repressed by glucose and is induced only under respiratory conditions or during the stationary phase (36), whereas transcription of *GDH1* in cells grown with glucose is regulated by the transcriptional activators Gln3, Hap2, and Hap3 (37).

To determine whether the transcription profiles of *GDH1* and *GDH3* are consistent with the subsequent gene expression events, we analyzed the enzymatic activities and protein levels of Gdh1 and Gdh3 in WT cells and a variety of mutant strains. The levels of NADP-GDH activity in the exponential phase (24 h) cells of Δ*gdh3*, Δ*gdh1*Δ*gdh3*/YCpGdh1, and WT strains were ~10-fold higher than in Δ*gdh1* and Δ*gdh1*Δ*gdh3*/YCpGdh3 cells. Meanwhile, the levels of NADP-GDH activity in the stationary phase (48 h) cells of Δ*gdh1*, Δ*gdh1*Δ*gdh3*/YCpGdh3, and WT strains were at least seven times higher than in Δ*gdh3* and Δ*gdh1*Δ*gdh3*/YCpGdh1 cells (Table 4). In immunoblotting, Gdh1 protein was detected in the exponential phase (24 h) cells of Δ*gdh3*, Δ*gdh1*Δ*gdh3*/YCpGdh1, and WT strains but not in the stationary phase (48 h) cells of the strains (Fig. 6*A*). On the contrary, Gdh3 protein was detected in the stationary phase cells of Δ*gdh1*, Δ*gdh1*Δ*gdh3*/YCpGdh3, and WT strains but not in their exponential phase cells. In addition, a substantial level of Gdh1-FLAG signal was detected in Δ*gdh1*Δ*gdh3*/YCpGdh1-FLAG cells during the exponential phase (12 and 24 h), but no signal was identified during the stationary phase (48 and 72 h) (Fig. 6*B*). However, Δ*gdh1*Δ*gdh3*/YCpGdh3-FLAG cells showed only negligible levels of Gdh3-FLAG signal during the logarithmic phase followed by a marked increase in Gdh3-FLAG signal to the highest level during stationary phase. Together, these results suggest that a large majority of the NADP-GDH activity is Gdh1-dependent until the cells reach late logarithmic phase and then becomes Gdh3-dependent during the stationary phase.

Gdh1, but Not Gdh3, Is Subjected to Degradation in Stationary Phase Cells in Which the Lys-426 Residue Plays an Essential Role—Interestingly, the results of the NADP-GDH activity assays (Table 4) and immunoblotting (Fig. 6) obtained from the stationary phase cells exhibited a significant discrepancy with the results of the β-gal reporter assay (Fig. 5) in that only negligible levels of Gdh1 protein and its corresponding NADP-GDH activity were detected despite relatively high levels of *GDH1* transcription. To further investigate the cause for such discrepancy, we monitored the activity and protein levels of NADP-GDH in Δ*gdh1*Δ*gdh3* cells carrying either of the promoter-swapped derivatives of *GDH1* or *GDH3*. Although the levels of NADP-GDH activity in the $YCpP_{GDH1}$-Gdh3 transformants were almost the same as those in the WT cells regardless of growth stage, the NADP-GDH activity in cells carrying $YCpP_{GDH3}$-Gdh1 was negligible (Table 4). Accordingly, no signal for the Gdh1-FLAG protein was detected in Δ*gdh1*Δ*gdh3*/$YCpP_{GDH3}$-Gdh1-FLAG cells throughout all growth stages, whereas strong signals for the FLAG-tagged Gdh3-FLAG protein was observed in Δ*gdh1*Δ*gdh3*/$YCpP_{GDH1}$-Gdh3-FLAG cells in all growth stages (Fig. 6*B*). In agreement with these results, both the late logarithmic (24 h) and stationary (48 h) cells of the Δ*gdh1*Δ*gdh3*/$YCpP_{GDH1}$-Gdh3 transformant had levels of survival after a 1-h exposure to 10 mM H_2O_2 similar to those of WT cells, whereas the survival rates of Δ*gdh1*Δ*gdh3*/$YCpP_{GDH3}$-Gdh1 cells showed only basal levels of resistance against oxidative stress (Fig. 7). This result indicates that ectopic expression of $gdh1_P$::$gdh3_{ORF}$ confers consistent resistance to stress-induced apoptosis in Δ*gdh1*Δ*gdh3* cells throughout all growth stages, whereas the ectopic expression of $gdh3_P$::$gdh1_{ORF}$ cannot protect the cells from stress-induced damage. Taken together, these results suggest that the Gdh3 protein is stable throughout all growth stages, whereas Gdh1 is subjected to stationary phase-specific degradation.

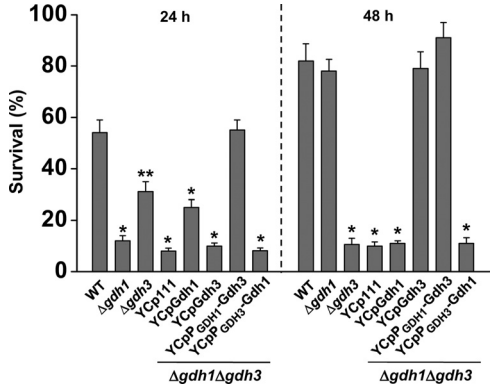

FIGURE 7. **Ectopic expression of $gdh3_P$::$gdh1_{ORF}$ cannot prevent stress-induced apoptosis in Δ*gdh1*Δ*gdh3* cells, whereas ectopic expression of $gdh1_P$::$gdh3_{ORF}$ confers stress resistance throughout all growth stages.** Yeast strains (WT, Δ*gdh1*, Δ*gdh3*, Δ*gdh1*Δ*gdh3*, Δ*gdh1*Δ*gdh3*/YCpGDH1, Δ*gdh1*Δ*gdh3*/YCpGDH3, Δ*gdh1*Δ*gdh3*/$YCpP_{GDH1}$-GDH3, and Δ*gdh1*Δ*gdh3*/$YCpP_{GDH3}$-GDH1) grown in SCD for 24 or 48 h were exposed to oxidative stress (10 mM H_2O_2, 1 h). Surviving cells were evaluated by CFU assays. Values are the mean ± S.E. of three independent experiments. *, $p < 0.001$; **, $p < 0.005$ (two-tailed Student's *t* test *versus* WT).

Gdh1 and Gdh3 share an extremely high degree of homology (~92%) over the entire amino acid sequences except for the $Box420_{Gdh1}$ and $Box420_{Gdh3}$ regions located near the C-terminal ends of the proteins (Fig. 8*A*). The most distinctive feature of $Box420_{Gdh1}$ is that it has four lysine residues that may be responsible for protein degradation, whereas $Box420_{Gdh3}$ contains only one lysine residue. Thus, to determine the mechanism of stationary phase-specific Gdh1 degradation, we constructed transformants carrying ectopic hybrid genes encoding the FLAG-tagged Gdh1 derivatives with single alanine (Ala) substitutions for lysine (Lys) in the $Box420_{Gdh1}$ region ($YCpGdh1_{K419A}$-FLAG, $YCpGdh1_{K420A}$-FLAG, $YCpGdh1_{K423A}$-FLAG, and $YCpGdh1_{K426A}$-FLAG) and tracked the quantitative change of the fusion proteins by immunoblotting. Although the $Gdh1_{K419A}$-FLAG, $Gdh1_{K420A}$-FLAG, and $Gdh1_{K423A}$-FLAG proteins were detected only in

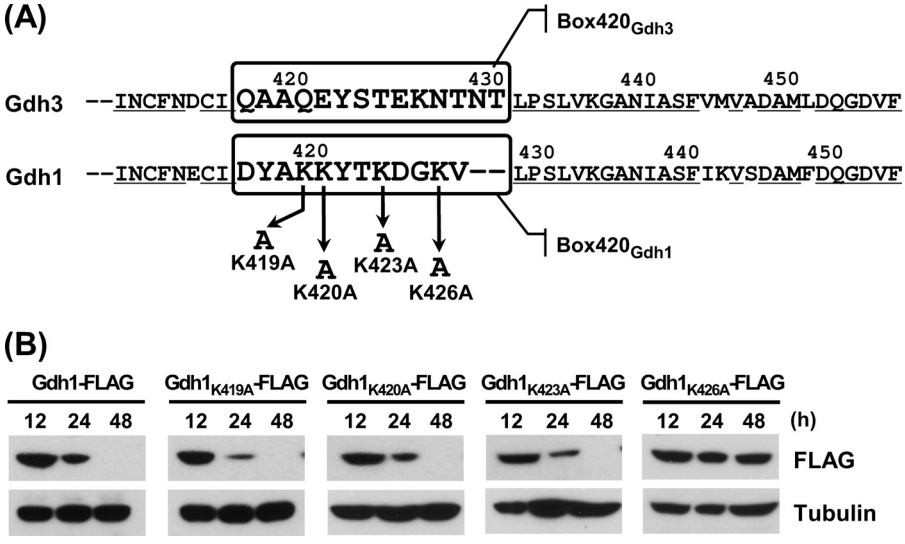

FIGURE 8. **Gdh1, but not Gdh3, is subjected to stationary phase-specific degradation in which the Lys-426 residue in the $Box420_{Gdh1}$ region plays an essential role.** *A*, amino acid sequences of the C-terminal regions of Gdh1 and Gdh3. The two isoenzymes share an extremely high degree of homology throughout their amino acid sequences except for in the $Box420_{Gdh1}$ and $Box420_{Gdh3}$ regions. Point mutations causing single amino acid substitutions in Gdh1 (K419A, K420A, K423A, and K426A) were introduced directly into YCpGdh1-FLAG. *B*, immunoblot analysis of the FLAG-tagged Gdh1 and its mutant derivatives. Yeast strains (BY4741) carrying $YCpGdh1_{K419A}$-FLAG, $YCpGdh1_{K420A}$-FLAG, $YCpGdh1_{K423A}$-FLAG, or $YCpGdh1_{K426A}$-FLAG were grown in SCD, and samples were taken after 12, 24, and 48 h of culture. Cell extracts were immunoblotted and probed with anti-FLAG and anti-tubulin antibodies.

exponential phase cells (12 and 24 h) as WT FLAG-tagged Gdh1 (Gdh1-FLAG), the $Gdh1_{K426A}$-FLAG protein was detected throughout all of the growth stages (Fig. 8*B*). Thus, the Lys-426 residue, but not Lys-419, Lys-420, or Lys-423, in the $Box420_{Gdh1}$ region plays an essential role in stationary phase-specific degradation of Gdh1.

DISCUSSION

S. cerevisiae is the first microorganism described in which the NADP-GDH activity is encoded by two genes (16). It has been claimed that coordinated regulation of the two NADP-GDH isoenzymes enables a balanced utilization of α-ketoglutarate for glutamate synthesis during diauxic growth and eventually improves the efficiency of glutamate biosynthesis (19). However, the physiological significance of this apparent redundancy has not yet been fully addressed. In the present study, we attempted to determine the differential role of the two isoforms of NADP-GDH, Gdh1 and Gdh3, in the resistance to stress-induced apoptosis and chronological aging.

The initial clue as to the involvement of Gdh3 in the protection against stress-induced apoptosis was based on the observation that Gdh3-null cells, but not Gdh1- or Gdh3-null cells, were hypersensitive to oxidative and thermal stress compared with WT cells (Fig. 1*A*). We observed several typical morphological and cytological hallmarks of apoptosis, such as ROS accumulation, nuclear and DNA fragmentation, and phosphatidylserine translocation, in stationary phase Gdh3-null cells following oxidative stress (Fig. 2). A similar phenomenon was observed in Gdh3-null cells exposed to thermal stress (data not shown). In addition, impairment of *GDH3* resulted in a higher susceptibility to chronological aging-induced cell death followed by regrowth of a subpopulation that consisted of cells better adapted to prolonged culture conditions (Fig. 1*B*).

Cells should be equipped with an efficient ROS-scavenging enzymatic system to protect against oxidative damage. Superoxide dismutase catalyzes the destruction of superoxide free radicals to oxygen and H_2O_2 (38), which is in turn reduced to H_2O by catalase or peroxidase. The principal enzyme for H_2O_2 detoxification is generally considered to be glutathione peroxidase (GPx), which requires GSH as a reducing power (39), rather than catalase, because catalase has a much lower affinity than GPx for H_2O_2 (40). Thus, GSH is an essential metabolite for stress resistance. When grown in SCD medium, Gdh3-null cells were subject to GSH depletion, which was relieved by an exogenous supply of GSH or glutamate (Table 3). Furthermore, the hypersusceptibility of the stationary cells of Gdh3-null strains to thermal and oxidative stress-induced apoptosis, which is mediated by ROS, was suppressed by exogenous GSH or glutamate (Fig. 3) or by deletion of *GDH2* (Fig. 4). Thus, Gdh3 plays a pivotal role in preventing the stress-induced ROS accumulation and subsequent apoptotic events by supplying glutamate, one of the precursors for GSH biosynthesis, in stationary phase cells. It is also suggested that the major form of the ROS accumulated in the stationary phase Gdh3-null cells exposed to oxidative and thermal stress is H_2O_2, the substrate of GPx. In a human B-lymphoma cell line, decreased GSH alone can act as a potent early activator of apoptotic signaling. Increased ROS production following mitochondrial GSH depletion irreversibly commits cells to apoptosis (41). In addition, both glutamate and glutamine have a significant role not only in the resistance of cells to apoptosis but also in promoting cell proliferation (42). Glutamate can rescue a breast carcinoma cell line from apoptotic cell death (43). Taken together, in both yeast and mammalian cells, glutamate is required for the first committed step in the synthesis of GSH and acts as a suppressor of stress-induced apoptosis. Thus, the present results indicate that yeast strains lacking NADP-GDH could be used as a model system for studying the mechanisms of apoptotic or proliferative defects related to glutamate metabolism in mammals.

Despite the high level of sequence homology between Gdh1 and Gdh3, the transcription patterns of *GDH1* and *GDH3* are significantly different from each other. Our data from the β-gal reporter assays indicate that *GDH3* transcription occurs mainly during the stationary phase, whereas *GDH1* is transcribed consistently throughout all growth periods (Fig. 5). Accordingly, *GDH3* transcription is strongly repressed by glucose and is highly induced under respiratory conditions and during the stationary phase (36, 37, 44). This implies that Gdh3 may play a crucial role in sustaining oxidative phosphorylation. On the other hand, *GDH1* transcription is controlled by transcriptional activators exclusive of either nitrogen (Gln3 and Gcn4) or carbon metabolism (HAP complex) and occurs independently of growth stage and glucose repression (37).

Although consistently high levels of *GDH1* transcription were observed regardless of the growth stage (Fig. 5), negligible levels of Gdh1 protein (Fig. 6*A*) and its NADP-GDH activity (Table 4) were detected during the stationary phase, suggesting that Gdh1 is subjected to stationary phase-specific degradation. The activity and protein levels of the NADP-GDH in Δ*gdh1*Δ*gdh3* cells carrying ectopic copies of the promoter-swapped derivatives of *GDH1* or *GDH3* were in agreement with our hypothesis: whereas the NADP-GDH activity of Gdh3 ($YCpP_{GDH1}$-Gdh3) and the protein level of Gdh3-FLAG ($YCpP_{GDH1}$-Gdh3-FLAG) were consistently high, the NADP-GDH activity of Gdh1 ($YCpP_{GDH3}$-Gdh1) and Gdh1-FLAG ($YCpP_{GDH3}$-Gdh1-FLAG) protein levels were trivial throughout all growth periods (Table 4 and Fig. 6*B*). In further support, a previous study reported that transfer of *S. cerevisiae* cultures to medium deficient in a readily utilizable carbon source results in proteolysis of NADP-GDH. However, it has not been determined which of the two NADP-GDH, Gdh1 or Gdh3, is subjected to such degradation (20).

We asked how it is that only Gdh1, but not Gdh3, is subjected to stationary phase-specific degradation despite the extremely high degree of sequence homology between the two enzymes. Thus, we evaluated the importance of degradation of the lysine-rich Box420 region of Gdh1 ($Box420_{Gdh1}$) that contains a sequence distinct from that of the corresponding Box420 region of Gdh3 ($Box420_{Gdh3}$) (Fig. 8*A*). Substituting alanine for the lysine residues in $Box420_{Gdh1}$ and tracking the stability of the mutant derivatives of Gdh1 revealed that only one lysine residue (Lys-426) of the four lysine residues concentrated in $Box420_{Gdh1}$ was necessary for the stationary phase-specific degradation of Gdh1 (Fig. 8). A previous study identified Lys-325 and Lys-371 of Gdh1 as ubiquitinated residues through a proteomics approach to enrich, recover, and identify ubiquitin

conjugates from *S. cerevisiae* lysates (45). Although almost all of the ubiquitin-modified lysine residues are exposed at the surface of the molecule and are readily accessible from the outside, Lys-371 is located in a hydrophobic stretch, PPKAA, and is buried inside the protein (46). Thus, this position may be involved in the degradation of misfolded Gdh1 molecules. However, Gdh1 and Gdh3 share a striking homology throughout their amino acid sequences, except for their Box420 regions. The sequences surrounding Lys-325 and Lys-371 in Gdh1 are almost identical to those centered at the corresponding lysine residues, Lys-326 and Lys-372, in Gdh3. Thus neither of the lysine residues is responsible for the stationary phase-specific degradation of Gdh1. The significance of the ubiquitination of Lys-325 and Lys-371 requires further investigation. Future studies will focus on determining whether the degradation of Gdh1 is mediated by the ubiquitin-proteosome pathway in which Lys-426 provides a specific binding site for ubiquitin.

During the stationary phase, yeast cells acquire a variety of features, including a dramatic reduction in the overall rate of growth and protein synthesis, accumulation of the storage carbohydrate glycogen, and increased resistance to a variety of environmental stresses such as oxidative stress and heat shock (47, 48). Specifically, the rate of protein synthesis drops ~300-fold upon entry into stationary phase (48, 49), which is an essential characteristic for stationary phase survival (50). Thus, it seems that a variety of amino acids become unnecessary for protein synthesis in stationary phase cells. In parallel, cells protect themselves from increasing environmental stress-induced accumulation of ROS during stationary phase. Among the ROS-scavenging systems, the GSH system, which consists of GSH, GPx, and glutathione reductase, is probably the most important intracellular defense mechanism. GPx catalyzes the reduction of H_2O_2 and oxidizes GSH to GSSG. GSSG is then reduced back to GSH by glutathione reductase. Hence, the ability of the cell to reduce GSSG or synthesize GSH from glutamate is the key to how effectively the cell can eliminate ROS-mediated cell damage (51). In our previous study, we showed that the hypersusceptibility of yeast cells lacking Cit1 to stress-induced apoptosis mediated by ROS does not result from the depletion of reducing power required for glutathione reductase reaction but, instead, is due to an insufficient supply of glutamate, a precursor of GSH biosynthesis (31). Therefore, yeast cells in stationary phase require glutamate for their GSH supply rather than for protein synthesis. The two isofunctional NADP-GDH of *S. cerevisiae* differ in allosteric properties and rates of α-ketoglutarate utilization. Specifically, Gdh1 exhibits a 3-fold higher rate of α-ketoglutarate utilization than does Gdh3 (19). Thus, Gdh1 is more suitable for functioning as a major glutamate-producing enzyme during the exponential phase in which substantial amounts of amino acids, including glutamate, are necessary for protein synthesis. On the other hand, Gdh3 seems to be more suitable during the stationary phase in which glutamate is mainly required for GSH biosynthesis. Therefore, it may be more beneficial to the cells to substitute Gdh1 with Gdh3 through the stationary phase-specific expression of *GDH3* and simultaneous degradation of Gdh1 after exiting from the exponential growth phase.

Acknowledgments—We thank Profs. Jeong-Yoon Kim and Hee-Moon Park for critical reading of the manuscript and valuable advice.

REFERENCES

1. Hudson, R. C., and Daniel, R. M. (1993) L-Glutamate dehydrogenases: distribution, properties, and mechanism. *Comp. Biochem. Physiol. B* **106,** 767–792
2. McKenna, M. C., Sonnewald, U., Huang, X., Stevenson, J., and Zielke, H. R. (1996) Exogenous glutamate concentration regulates the metabolic fate of glutamate in astrocytes. *J. Neurochem.* **66,** 386–393
3. Plaitakis, A., and Zaganas, I. (2001) Regulation of human glutamate dehydrogenases: implications for glutamate, ammonia, and energy metabolism in brain. *J. Neurosci. Res.* **66,** 899–908
4. Cooper, A. J., and Plum, F. (1987) Biochemistry and physiology of brain ammonia. *Physiol. Rev.* **67,** 440–519
5. Plaitakis, A., Metaxari, M., and Shashidharan, P. (2000) Nerve tissue-specific (GLUD2) and housekeeping (GLUD1) human glutamate dehydrogenases are regulated by distinct allosteric mechanisms: implications for biologic function. *J. Neurochem.* **75,** 1862–1869
6. Mavrothalassitis, G., Tzimagiorgis, G., Mitsialis, A., Zannis, V., Plaitakis, A., Papamatheakis, J., and Moschonas, N. (1988) Isolation and characterization of cDNA clones encoding human liver glutamate dehydrogenase: evidence for a small gene family. *Proc. Natl. Acad. Sci. U.S.A.* **85,** 3494–3498
7. Shashidharan, P., Michaelidis, T. M., Robakis, N. K., Kresovali, A., Papamatheakis, J., and Plaitakis, A. (1994) Novel human glutamate dehydrogenase expressed in neural and testicular tissues and encoded by an X-linked intronless gene. *J. Biol. Chem.* **269,** 16971–16976
8. Fahien, L. A., MacDonald, M. J., Kmiotek, E. H., Mertz, R. J., and Fahien, C. M. (1988) Regulation of insulin release by factors that also modify glutamate dehydrogenase. *J. Biol. Chem.* **263,** 13610–13614
9. Sener, A., Malaisse-Lagae, F., and Malaisse, W. J. (1981) Stimulation of pancreatic islet metabolism and insulin release by a nonmetabolizable amino acid. *Proc. Natl. Acad. Sci. U.S.A.* **78,** 5460–5464
10. Stanley, C. A., Lieu, Y. K., Hsu, B. Y., Burlina, A. B., Greenberg, C. R., Hopwood, N. J., Perlman, K., Rich, B. H., Zammarchi, E., and Poncz, M. (1998) Hyperinsulinism and hyperammonemia in infants with regulatory mutations of the glutamate dehydrogenase gene. *N. Engl. J. Med.* **338,** 1352–1357
11. Haigis, M. C., Mostoslavsky, R., Haigis, K. M., Fahie, K., Christodoulou, D. C., Murphy, A. J., Valenzuela, D. M., Yancopoulos, G. D., Karow, M., Blander, G., Wolberger, C., Prolla, T. A., Weindruch, R., Alt, F. W., and Guarente, L. (2006) SIRT4 inhibits glutamate dehydrogenase and opposes the effects of calorie restriction in pancreatic beta cells. *Cell* **126,** 941–954
12. Shashidharan, P., Clarke, D. D., Ahmed, N., Moschonas, N., and Plaitakis, A. (1997) Nerve tissue-specific human glutamate dehydrogenase that is thermolabile and highly regulated by ADP. *J. Neurochem.* **68,** 1804–1811
13. Zaganas, I., Kanavouras, K., Mastorodemos, V., Latsoudis, H., Spanaki, C., and Plaitakis, A. (2009) The human GLUD2 glutamate dehydrogenase: localization and functional aspects. *Neurochem. Int.* **55,** 52–63
14. Plaitakis, A., Latsoudis, H., and Spanaki, C. (2011) The human GLUD2 glutamate dehydrogenase and its regulation in health and disease. *Neurochem. Int.* **59,** 495–509
15. Miller, S. M., and Magasanik, B. (1990) Role of NAD-linked glutamate dehydrogenase in nitrogen metabolism in *Saccharomyces cerevisiae*. *J. Bacteriol.* **172,** 4927–4935
16. Avendaño, A., Deluna, A., Olivera, H., Valenzuela, L., and Gonzalez, A. (1997) GDH3 encodes a glutamate dehydrogenase isozyme, a previously unrecognized route for glutamate biosynthesis in *Saccharomyces cerevisiae*. *J. Bacteriol.* **179,** 5594–5597
17. Benjamin, P. M., Wu, J. I., Mitchell, A. P., and Magasanik, B. (1989) Three regulatory systems control expression of glutamine synthetase in *Saccharomyces cerevisiae* at the level of transcription. *Mol. Gen. Genet.* **217,** 370–377
18. Filetici, P., Martegani, M. P., Valenzuela, L., González, A., and Ballario, P. (1996) Sequence of the *GLT1* gene from *Saccharomyces cerevisiae* reveals

the domain structure of yeast glutamate synthase. *Yeast* **12,** 1359–1366
19. DeLuna, A., Avendano, A., Riego, L., and Gonzalez, A. (2001) NADP-glutamate dehydrogenase isoenzymes of *Saccharomyces cerevisiae*. Purification, kinetic properties, and physiological roles. *J. Biol. Chem.* **276,** 43775–43783
20. Mazón, M. J., and Hemmings, B. A. (1979) Regulation of *Saccharomyces cerevisiae* nicotinamide adenine dinucleotide phosphate-dependent glutamate dehydrogenase by proteolysis during carbon starvation. *J. Bacteriol.* **139,** 686–689
21. Ito, H., Fukuda, Y., Murata, K., and Kimura, A. (1983) Transformation of intact yeast cells treated with alkali cations. *J. Bacteriol.* **153,** 163–168
22. Madeo, F., Fröhlich, E., and Fröhlich, K. U. (1997) A yeast mutant showing diagnostic markers of early and late apoptosis. *J. Cell Biol.* **139,** 729–734
23. Wu, C. Y., Bird, A. J., Winge, D. R., and Eide, D. J. (2007) Regulation of the yeast TSA1 peroxiredoxin by ZAP1 is an adaptive response to the oxidative stress of zinc deficiency. *J. Biol. Chem.* **282,** 2184–2195
24. Cogoni, C., Valenzuela, L., González-Halphen, D., Olivera, H., Macino, G., Ballario, P., and González, A. (1995) *Saccharomyces cerevisiae* has a single glutamate synthase gene coding for a plant-like high-molecular-weight polypeptide. *J. Bacteriol.* **177,** 792–798
25. Doherty, D. (1970) L-Glutamate dehydrogenase (yeast). *Methods Enzymol.* **17,** 850–856
26. Lowry, O. H., Rosebrough, N. J., Farr, A. L., and Randall, R. J. (1951) Protein measurement with the Folin phenol reagent. *J. Biol. Chem.* **193,** 265–275
27. Anderson, M. E. (1985) Determination of glutathione and glutathione disulfide in biological samples. *Methods Enzymol.* **113,** 548–555
28. Lauber, K., Appel, H. A., Schlosser, S. F., Gregor, M., Schulze-Osthoff, K., and Wesselborg, S. (2001) The adapter protein apoptotic protease-activating factor-1 (Apaf-1) is proteolytically processed during apoptosis. *J. Biol. Chem.* **276,** 29772–29781
29. Fabrizio, P., Battistella, L., Vardavas, R., Gattazzo, C., Liou, L. L., Diaspro, A., Dossen, J. W., Gralla, E. B., and Longo, V. D. (2004) Superoxide is a mediator of an altruistic aging program in *Saccharomyces cerevisiae*. *J. Cell Biol.* **166,** 1055–1067
30. Fabrizio, P., and Longo, V. D. (2003) The chronological life span of *Saccharomyces cerevisiae*. *Aging Cell* **2,** 73–81
31. Lee, Y. J., Hoe, K. L., and Maeng, P. J. (2007) Yeast cells lacking the CIT1-encoded mitochondrial citrate synthase are hypersusceptible to heat- or aging-induced apoptosis. *Mol. Biol. Cell* **18,** 3556–3567
32. Madeo, F., Fröhlich, E., Ligr, M., Grey, M., Sigrist, S. J., Wolf, D. H., and Fröhlich, K. U. (1999) Oxygen stress: a regulator of apoptosis in yeast. *J. Cell Biol.* **145,** 757–767
33. Mayor, T., Lipford, J. R., Graumann, J., Smith, G. T., and Deshaies, R. J. (2005) Analysis of polyubiquitin conjugates reveals that the Rpn10 substrate receptor contributes to the turnover of multiple proteasome targets. *Mol. Cell. Proteomics* **4,** 741–751
34. Grant, C. M., MacIver, F. H., and Dawes, I. W. (1996) Glutathione is an essential metabolite required for resistance to oxidative stress in the yeast *Saccharomyces cerevisiae*. *Curr. Genet.* **29,** 511–515
35. Grant, C. M. (2001) Role of the glutathione/glutaredoxin and thioredoxin systems in yeast growth and response to stress conditions. *Mol. Microbiol.* **39,** 533–541
36. Avendaño, A., Riego, L., DeLuna, A., Aranda, C., Romero, G., Ishida, C., Vázquez-Acevedo, M., Rodarte, B., Recillas-Targa, F., Valenzuela, L., Zonszein, S., and González, A. (2005) Swi/SNF-GCN5-dependent chromatin remodelling determines induced expression of GDH3, one of the paralogous genes responsible for ammonium assimilation and glutamate biosynthesis in *Saccharomyces cerevisiae*. *Mol. Microbiol.* **57,** 291–305
37. Riego, L., Avendaño, A., DeLuna, A., Rodríguez, E., and González, A. (2002) GDH1 expression is regulated by GLN3, GCN4, and HAP4 under respiratory growth. *Biochem. Biophys. Res. Commun.* **293,** 79–85
38. Bermingham-McDonogh, O., Gralla, E. B., and Valentine, J. S. (1988) The copper, zinc-superoxide dismutase gene of *Saccharomyces cerevisiae*: cloning, sequencing, and biological activity. *Proc. Natl. Acad. Sci. U.S.A.* **85,** 4789–4793
39. Galiazzo, F., Schiesser, A., and Rotilio, G. (1987) Glutathione peroxidase in yeast. Presence of the enzyme and induction by oxidative conditions. *Biochem. Biophys. Res. Commun.* **147,** 1200–1205
40. Avery, A. M., and Avery, S. V. (2001) *Saccharomyces cerevisiae* expresses three phospholipid hydroperoxide glutathione peroxidases. *J. Biol. Chem.* **276,** 33730–33735
41. Armstrong, J. S., Steinauer, K. K., Hornung, B., Irish, J. M., Lecane, P., Birrell, G. W., Peehl, D. M., and Knox, S. J. (2002) Role of glutathione depletion and reactive oxygen species generation in apoptotic signaling in a human B lymphoma cell line. *Cell Death Differ.* **9,** 252–263
42. Matés, J. M., Pérez-Gómez, C., Núñez de Castro, I., Asenjo, M., and Márquez, J. (2002) Glutamine and its relationship with intracellular redox status, oxidative stress, and cell proliferation/death. *Int. J. Biochem. Cell Biol.* **34,** 439–458
43. Savolainen, K. M., Loikkanen, J., and Naarala, J. (1995) Amplification of glutamate-induced oxidative stress. *Toxicol. Lett.* **82,** 399–405
44. Cox, K. H., Tate, J. J., and Cooper, T. G. (2002) Cytoplasmic compartmentation of Gln3 during nitrogen catabolite repression and the mechanism of its nuclear localization during carbon starvation in Saccharomyces cerevisiae. *J. Biol. Chem.* **277,** 37559–37566
45. Mayor, T., and Deshaies, R. J. (2005) Two-step affinity purification of multiubiquitylated proteins from *Saccharomyces cerevisiae*. *Methods Enzymol.* **399,** 385–392
46. Catic, A., Collins, C., Church, G. M., and Ploegh, H. L. (2004) Preferred *in vivo* ubiquitination sites. *Bioinformatics* **20,** 3302–3307
47. Werner-Washburne, M., Braun, E., Johnston, G. C., and Singer, R. A. (1993) Stationary phase in the yeast *Saccharomyces cerevisiae*. *Microbiol. Rev.* **57,** 383–401
48. Werner-Washburne, M., Braun, E. L., Crawford, M. E., and Peck, V. M. (1996) Stationary phase in *Saccharomyces cerevisiae*. *Mol. Microbiol.* **19,** 1159–1166
49. Herman, P. K. (2002) Stationary phase in yeast. *Curr. Opin. Microbiol.* **5,** 602–607
50. Paz, I., and Choder, M. (2001) Eukaryotic translation initiation factor 4E-dependent translation is not essential for survival of starved yeast cells. *J. Bacteriol.* **183,** 4477–4483
51. Wang, X. F., and Cynader, M. S. (2000) Astrocytes provide cysteine to neurons by releasing glutathione. *J. Neurochem.* **74,** 1434–1442